

BSAlign: a library for nucleotide sequence alignment

Haojing Shao^{a,b}, Jue Ruan^{a,b,c}

^a*Shenzhen Branch, Guangdong Laboratory of Lingnan Modern Agriculture, Genome Analysis Laboratory of the Ministry of Agriculture and Rural Affairs, Agricultural Genomics Institute at Shenzhen, Chinese Academy of Agricultural Sciences, No 7, Pengfei Road, Dapeng District, Shenzhen, 518120, Guangdong, China*

^b*Contributed equally.*

^c*Corresponding author. E-mail: ruanjue@caas.cn,*

Abstract

Increasing the accuracy of the nucleotide sequence alignment is an essential issue in genomics research. Although classic dynamic-programming algorithms (e.g., Smith-Waterman and Needleman–Wunsch) guarantee to produce the optimal result, their time complexity hinders the application of large-scale sequence alignment. Many optimization efforts that aim to accelerate the alignment process generally come from three perspectives: re-designing data structures (e.g., diagonal or striped Single Instruction Multiple Data (SIMD) implementations), increasing the number of parallelisms in SIMD operations (e.g., difference recurrence relation), or reducing searching space (e.g., banded dynamic programming). However, no methods combine all these three aspects to build an ultra-fast algorithm. We have developed a Banded Striped Aligner(library) named BSAlign that delivers accurate alignment results at an ultra-fast speed by knitting a series of novel methods together to take advantage of all of the aforementioned three perspectives with highlights such as active F-loop in striped vectorization and striped move in banded dynamic programming. We applied our new acceleration design on both regular and edit-distance pairwise alignment. BSAlign achieved 2-fold speedup than other SIMD based implementations for regular pairwise alignment, and 1.5 to 4-fold speedup in edit distance based implementations for long reads. BSAlign is implemented in C programing language and is available at <https://github.com/ruanjue/bsalign>.

Keywords: keyword one, keyword two Pairwise alignment, Edit distance, striped vectorization, banded dynamic programming, F evaluation

1. Introduction

2 Nucleotide sequence alignment is a way to arrange and compare
3 DNA/RNA sequences from different sources to identify their regions of sim-
4 ilarity. Two classic algorithms, namely Needleman-Wunsch algorithm[1] and
5 Smith-Waterman algorithm[2], are commonly used for sequence alignment.
6 They handle sequence alignment by solving a dynamic programming problem
7 in which a scoring matrix is calculated and an optimal path from the cell with
8 a maximal score is returned. Although these two methods have shown high
9 capability in finding optimal alignment results, they require quadratic time
10 complexity and rapidly degenerate especially when processing long sequences.
11 To accelerate the alignment process, three major categories of optimization
12 techniques have been developed along the way.

13 *Single Instruction Multiple Data (SIMD)*. The first optimization cate-
14 gory is to re-design the data structure of the scoring matrix calculation to
15 resolve data dependencies between neighboring cells so that the conditional
16 branch within the inner loop of the dynamic programming algorithm can
17 be eliminated and hence more efficient in parallelization techniques such as
18 SIMD. Among the initial trials in this category, Wozniak[3] has presented an
19 implementation to store values parallel to the minor diagonal to eliminate
20 the conditional branch in the inner loop of traditional implementation and
21 achieved a 2x speedup. In a different trial, Rognes et al.[4] introduced another
22 implementation to store values parallel to the query sequences. Compared to
23 Wozniak's implementation, an advantage of Rognes's design is that it only
24 needs to compute the query profile once for the entire reference sequences.
25 However, the disadvantage is that conditional branches are placed in the
26 inner loop when evaluating F matrix. The length of a single instruction
27 ranges from 128-bit to 512-bit for recent tools such as BGSA[5], SeqAn[6]
28 and AnySeq[7].

29 *Striped SIMD and F evaluation*. To combine the merits of both
30 Wozniak[3] and Rognes[4], Farrar[8] fixed these disadvantages by introduc-
31 ing a layout of query sequences that are parallel to the SIMD registers but
32 are accessed in a striped pattern, which only computes query profile once
33 and moves the conditional F matrix evaluation outside of the inner loop.
34 As a result, Farrar's striped vectorization successfully speeds up the Smith-
35 Waterman algorithm and has been adopted by many aligners, such as BWA-
36 SW[9], Bowtie2[10], and SSW library[11]. However, cells in the same register
37 are not always independent of each other. Farrar[8] solved this problem by

adding a correction loop for every F element, which may iterate many times when the indels are long enough.

Difference recurrence relation. The next optimization category is to increase the number of parallelisms in SIMD operations such as difference recurrence relation [12]. Since the traditional pairwise alignment stores and calculates the absolute values in the score matrix, it limits the width of SIMD operation as the sequence length increase. The difference recurrence relation solves this problem by only storing and calculating the differences between the adjacent cells, which keeps the full width of SIMD operation regardless of the sequence length. For example, the number of bits for storing the absolute value of a single cell is 16 or even 32. But it can reduce to 8 bits if just storing the differences between cells. Therefore, the number of parallelisms increases by 2 to 4 times.

Banded dynamic programming. Another optimization category is reducing the search space such as banded dynamic programming(DP). Instead of calculating the whole score matrix, banded DP maintains a hypothetical "band" around cells with maximal scores and only calculates the scores for cells within the "band" and skips calculating the remaining cells within the matrix[13, 14]. How to combine the method of using SIMD (minor diagonal or striped) and the idea of reducing the search space is not clear, especially when the input sequences contain abundant indel errors by third-generation sequencers. Suzuki et al.[14] proposed a minor diagonal SIMD adaptive banded DP algorithm, which is implemented and improved in a popular long read mapper minimap2[15]. Since the striped SIMD method[8] proved to be six times faster than the minor diagonal and other SIMD method[3] in SW algorithm without banded DP, the algorithm to combine the best SIMD method with banded DP is not developed yet.

Block aligner and wavefront algorithm. Recent methods block aligner(BA)[16] and wavefront algorithm(WFA)[17] manage to reduce the search space around the diagonal by two innovative approaches. Block aligner starts the alignment by a small square block and extends the block dynamically until the endpoint is reached. The block could be shifted either down or right according to the sum of the cells. The size of the extended block may double when a Y-drop condition is met. The width of the block (band) depends on the sequence's identity. Unlike the block aligner, the wavefront algorithm regards the global alignment as the wave spreading from the start point to the endpoint. WFA extends the wave step-by-step until the endpoint is reached. To speed up, WFA utilizes homologous region between the

76 sequences to skip the path(wavefront) that are unlikely to lead to the opti-
77 mal solution. The search space for the wavefront aligner is wave-like banding
78 along the diagonal.

79 Overall, we present a new library with an aligner, BSAlign, that is able
80 to combine merits from the aforementioned optimization techniques without
81 bringing their respective limitations. Firstly, we developed an active F loop
82 evaluation algorithm in the striped vectorization[8] to reduce the redundant F
83 matrix recalculation, which accelerates the evaluation of the scoring matrix.
84 We also introduced difference recurrence relation and developed a banded
85 DP striped move algorithm to efficiently combine the striped SIMD method
86 and banded DP. Finally, we designed a fast bit-vector algorithm to further
87 speed-up edit distance based alignment.

88 2. Materials and Methods

89 2.1. Overview

90 We developed a set of new methods to address the pairwise se-
91 quence alignment problem by adopting advantages from previous work like
92 striped vectorization [8], difference recurrence relation[12], banded dynamic
93 programming[13], and by proposing novel improvements like a technique
94 called active F-loop evaluation, a set of newly derived recurrence relations,
95 a variant of bit conversion for edit-distance alignment, and different levels of
96 adjustments to integrate all the features into the BSAlign.

97 2.2. The global alignment of nucleotide sequences

98 In the beginning, the algorithm calculates the global alignment by the
99 Needleman Wunsch algorithm[1]. The two sequences to be aligned, the query
100 sequence and the reference sequence, are defined as Q and R. The length of
101 the query sequence and reference sequence are then defined as Q_{len} and R_{len} ,
102 respectively. A matching matrix $S(q_i, r_j)$ is defined for all residue pairs (a, b)
103 where $a, b \in \{A, T, C, G\}$. The matching score $S(q_i, r_j) < 0$ when $q_i \neq r_j$ and
104 $S(q_i, r_j) > 0$ when $q_i == r_j$. The penalty for starting a gap and continuing
105 a gap are defined as GapO (gap open, $GapO < 0$), GapE (gap extension,
106 $GapE < 0$), and GapOE = GapO + GapE. We keep track of three scoring
107 matrices: E, F, and H, where E represents the alignment score ending with a

vertical gap, F represents the alignment score ending with a horizontal gap: 108

$$\begin{cases} E_{i,j} = \max\{E_{i,j-1} + \text{GapE}, H_{i,j-1} + \text{GapOE}\} \\ F_{i,j} = \max\{F_{i-1,j} + \text{GapE}, H_{i-1,j} + \text{GapOE}\} \\ H_{i,j} = \max\{E_{i,j}, F_{i,j}, H_{i-1,j-1} + S(q_i, r_j)\} \end{cases} \quad (1)$$

The cells for $H_{i,j}$, $E_{i,j}$ and $F_{i,j}$ are filled by 0 when $i < 1$ or $j < 1$. In 109
our implementation, we store $S(q_i, r_j)$ in four query profile arrays: $S(Q, A)$, 110
 $S(Q, C)$, $S(Q, T)$ and $S(Q, G)$. We calculate the score matrix row by row and 111
extract the $S(q_i, r_j)$ from query profile column $S(Q, r_j)$. We simplify $S(q_i, r_j)$ 112
as $S_{i,j}$ in this manuscript. 113

2.3. The striped SIMD data structure 114

To accelerate the pairwise alignment in the data structure, we first 115
implemented striped SIMD[8] to the row of the score matrix as well as the 116
query profile arrays. Assuming the query and reference sequences are the 117
row and column in the score matrix, respectively. The row is divided into 118
equal length segments, S . The number of segments, p , is equal to the number 119
of cells being processed in a SIMD register. Take an example in 128 SSE. 120
When processing byte integers (8-bit values) $p = 16$ and when processing 121
word integers (16-bit values) $p = 8$. Hence, p is fixed in the algorithm and 122
 S depends on query length (or band width) Q_{len} : $S = \lceil Q_{len}/p \rceil$ (Fig1a). 123
We first introduce the way to store the non-striped score matrix for each 124
register N in the memory: 125

$$\begin{aligned} N_0 &= [H_0, H_1, H_2, \dots, H_{p-1}] \\ N_1 &= [H_p, H_{p+1}, H_{p+2}, \dots, H_{p+p-1}] \\ &\dots \\ N_{S-1} &= [H_{p*(S-1)}, H_{p*(S-1)+1}, H_{p*(S-1)+2}, \dots, H_{p*(S-1)+p-1}] \end{aligned}$$

The potential overflow cells in N_{S-1} are filled by minimum value. In the 126
standard coordinate, there is an inner loop to compute H and F for each 127
register. 128

After striped conversion, the memory will store the score matrix for each 129
register M : 130

$$\begin{aligned} M_0 &= [H_0, H_{0+S}, H_{0+S*2}, \dots, H_{0+S*(p-1)}] \\ M_1 &= [H_1, H_{1+S}, H_{1+S*2}, \dots, H_{1+S*(p-1)}] \\ &\dots \\ M_{S-1} &= [H_{S-1}, H_{S-1+S}, H_{S-1+S*2}, \dots, H_{S-1+S*(p-1)}] \end{aligned}$$

131 Hence, the equation to convert each value ($N_{i,j}$) in non-striped SIMD(N) to
 132 any value ($M_{i,j}$) in striped SIMD(M) is:

$$N_{i,j} = M_{(i \% S) * p + \lfloor i/S \rfloor, j} \quad (2)$$

133 In the striped coordinate, all the inner loops to compute H and F are moved
 134 outside of the register. Now, M_{i+1} depends on M_i . The initial one M_0 is
 135 solved by the active F loop in the below subsection.

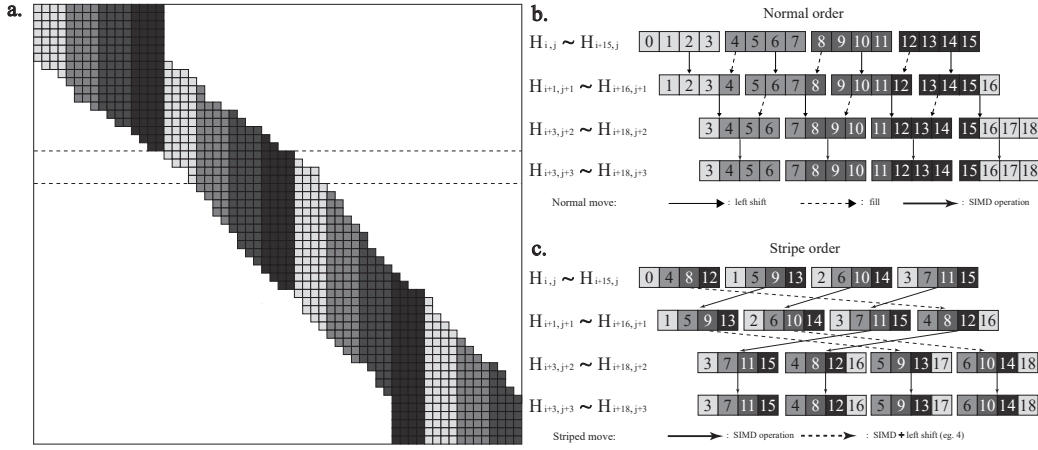


Figure 1: **The striped move algorithm for each row.** (a) Global visualization for the banded along the diagonal. (b) Detail example for row iteration in normal order. (c) Detail example for row iteration in striped order (striped move). Assuming the band width, the number of divided segments (S) and the number of cells (p) in a register are 16, 4 and 4, respectively. In normal order, the cells are in the same color for the same register. Only the offset is numbered inside the cell.

136 *2.4. The striped move algorithm for banded DP*

137 Another way to optimize the pairwise alignment is only focusing on the
 138 alignment along a diagonal band. A difficulty in applying banded DP to
 139 the striped SIMD method is that the entire striped SIMD data structure
 140 rearranges each time the band moves along the diagonal (Fig1b). To overcome
 141 this difficulty, we develop a method to move the striped SIMD data structure
 142 for banded DP (Fig1c).

143 In normal coordinate, the whole register stores (Fig1b):

$$\begin{aligned}
 N_{0,j} &= [\quad H_{i+0,j}, \quad H_{i+1,j}, \quad H_{i+2,j}, \quad \dots, \quad H_{i+p-1,j} \quad] \\
 N_{1,j} &= [\quad H_{i+p+0,j}, \quad H_{i+p+1,j}, \quad H_{i+p+2,j}, \quad \dots, \quad H_{i+p+p-1,j} \quad] \\
 &\dots \\
 N_{\bar{S}-1,j} &= [\quad H_{i+(\bar{S}-1)*p+0,j}, \quad H_{i+(\bar{S}-1)*p+1,j}, \quad H_{i+(\bar{S}-1)*p+2,j}, \quad \dots, \quad H_{i+(\bar{S}-1)*p+p-1,j} \quad]
 \end{aligned}$$

i and *j* are the first column and row coordinate in the memory and 144
 $\bar{S} * p$ is the band width. In the banded DP, the movement of the current 145
row indicates the selection of the optimal path. Moving zero, one and two 146
cells to the right indicates one vertical gap, no gap and one horizontal gap, 147
respectively(Fig1a). In our banded dynamic programming algorithm, we 148
compare the H in the first and last register, move the current row zero, one 149
or two cells to the right according to the comparison and prepare for the next 150
row. In the next row, the start position $H_{i+x,j+1}$ depends on the current row 151
 $[H_{i,j} \dots H_{i+\bar{S}*p-1,j}]$ as following: 152

$$H_{i+x,j+1} = \begin{cases} H_{i,j+1}, & (\text{Sum}(N_{0,j}) > \text{Sum}(N_{\bar{S}-1,j})) \\ H_{i+1,j+1}, & (\text{Sum}(N_{0,j}) == \text{Sum}(N_{\bar{S}-1,j})) \\ H_{i+2,j+1}, & (\text{Sum}(N_{0,j}) < \text{Sum}(N_{\bar{S}-1,j})) \end{cases}$$

$H_{i+x,j+1}$ move zero, one and two cell(s) to the right are showed as row $j+3$, 153
 $j+1$ and $j+2$ in Fig1b and Fig1c, respectively. We develop our striped move 154
following the above equations. In striped coordinates, the whole register 155
stores: 156

$$\begin{aligned}
 M_{0,j} &= [\quad H_{i,j}, \quad H_{i+1*\bar{S},j}, \quad H_{i+2*\bar{S},j}, \quad \dots, \quad H_{i+(p-1)*\bar{S},j} \quad] \\
 M_{1,j} &= [\quad H_{i+1,j}, \quad H_{i+1+1*\bar{S},j}, \quad H_{i+1+2*\bar{S},j}, \quad \dots, \quad H_{i+1+(p-1)*\bar{S},j} \quad] \\
 &\dots \\
 M_{\bar{S}-1,j} &= [\quad H_{i+\bar{S}-1,j}, \quad H_{i+\bar{S}-1+1*\bar{S},j}, \quad H_{i+\bar{S}-1+2*\bar{S},j}, \quad \dots, \quad H_{i+\bar{S}-1+(p-1)*\bar{S},j} \quad]
 \end{aligned}$$

The memory stores all the register as $[M_{0,j}, M_{1,j}, M_{2,j}, \dots, M_{\bar{S}-1,j}]$. In the 157
striped order, the cell order for the first register in $j+1$ row (such as 158
 $[H_{1,j+1}, H_{5,j+1}, H_{9,j+1}, H_{13,j+1}]$) is the same as the first, second and third reg- 159
ister in the j row(such as $[H_{1,j}, H_{5,j}, H_{9,j}, H_{13,j}]$) for moving zero, one or two 160
cells to the right, respectively(Fig1c). This holds true for all the registers 161
except the last one or two registers. For the calculation of the next row, the 162

163 memory is the following:

$$memory = \begin{cases} [M_{0,j+1}, M_{1,j+1}, M_{2,j+1}, \dots, M_{\bar{S}-1,j+1}], & (Sum(M_{0,j}) > Sum(M_{\bar{S}-1,j})) \\ [M_{1,j+1}, M_{2,j+1}, \dots, M_{\bar{S}-1,j+1}, \bar{M}_{0,j+1}], & (Sum(M_{0,j}) == Sum(M_{\bar{S}-1,j})) \\ [M_{2,j+1}, \dots, M_{\bar{S}-1,j+1}, \bar{M}_{0,j+1}, \bar{M}_{1,j+1}], & (Sum(M_{0,j}) < Sum(M_{\bar{S}-1,j})) \end{cases} \quad (3)$$

164 For the exception, the new \bar{M} can be converted from the previous
 165 M (dash arrow in Fig1c, such as $[H_{1,j+1}, H_{5,j+1}, H_{9,j+1}, H_{13,j+1}]$ to
 166 $[H_{5,j+2}, H_{9,j+2}, H_{13,j+2}, H_{17,j+2}]$). Take $\bar{M}_{0,j+1}$ as an example:

$$\bar{M}_{0,j+1} = (M_{0,j} \ll l_{byte}) + [0, 0, \dots, -\infty] \quad (4)$$

167 l_{byte} is the byte length of H . As the row moves one cell to the right, the whole
 168 cells move from $[H_{i,j} \dots H_{i+\bar{S}*p-1,j}]$ to $[H_{i+1,j+1} \dots H_{i+\bar{S}*p,j+1}]$. The addition cell
 169 $H_{i+\bar{S}*p,j+1}$ is set as the negative infinity and filled in the register. The negative
 170 infinity indicates this boundary cell will not be selected by equation1. The
 171 banded algorithm skips the calculation of boundary cells to speed up the
 172 global alignment. Using our striped move method, the whole striped SIMD
 173 data only needs bit operations to prepare for a new row in banded DP.

174 *2.5. Difference Recurrence Relation*

175 The third way to optimize the pairwise alignment is to increase the num-
 176 ber of parallelisms (i.e., vector width) in SIMD operations. We choose to
 177 calculate the score matrix based on the difference recurrence relation[12] in-
 178 stead of the conventional stripped SIMD implementation[8]. We denote h , e ,
 179 f as the relative score of the H , E , F score matrices respectively. We also de-
 180 fine u matrix and v matrix to represent the vertical difference and horizontal
 181 difference within the H matrix, respectively.

$$\begin{cases} h_{i,j} = H_{i,j} - H_{i-1,j-1} \\ u_{i,j} = H_{i,j} - H_{i-1,j} = h_{i,j} - v_{i-1,j} \\ v_{i,j} = H_{i,j} - H_{i,j-1} = h_{i,j} - u_{i,j-1} \\ e_{i,j} = E_{i,j} - H_{i,j-1} \\ f_{i,j} = F_{i,j} - H_{i-1,j-1} \end{cases} \quad (5)$$

182 The definition of e and f matrix is asymmetry. Under the above definition,
 183 our difference recurrence relation can be expressed as:

$$\begin{cases} h_{i,j} &= \max\{S_{i,j}, e_{i,j} + u_{i,j-1}, f_{i,j}\} \\ e_{i,j+1} &= \max\{e_{i,j} + u_{i,j-1} - h_{i,j} + \text{GapE}, \text{GapOE}\} \\ f_{i+1,j} &= \max\{f_{i,j} + \text{GapE}, h_{i,j} + \text{GapOE}\} - u_{i,j-1} \end{cases} \quad (6)$$

For every iteration in our implementation, we only store $u_{i,j-1}$ and $e_{i,j}$,
184 and calculate $h_{i,j}$, $v_{i,j}$, $e_{i,j+1}$ and $f_{i+1,j}$ by equation 5 and 6.
185

2.6. Active F loop

186

For non-striped pairwise alignment, the horizontal score F and its difference f can be calculated step-by-step via previous cells. In striped order, some cells show up before their previous cells(f_4, f_8, f_{12} in Fig2). Thus, it raises a problem only in calculating the horizontal score F and its difference f . Farrar[8] initially developed a lazy F evaluation method to solve this problem(Fig2a). It corrected the value F via a couple of loops, which is time-consuming for sequences that contain long indel errors(Fig2d). In contrast to lazy F evaluation, we actively correct all the cells in advance and guarantee that the value of H is always corrected, providing a linear complexity solution to this problem in any situation(Fig2b,2e).
187
188
189
190
191
192
193
194
195
196

For most registers in the memory, f is smaller than e and S . The value of H does not source from f (FigS1a). Only the horizontal gap will f start to influence the value of H (FigS1b,c). In the initial loop, we set the negative infinity as the first register $MF_{0,j}$ for horizontal difference $f([f_0 f_4 f_8 f_{12}]$ in Fig2e):
197
198
199
200
201

$$MF_{0,j} = [f_{0,j}, f_{\bar{S},j}, f_{\bar{S}*2,j}, \dots, f_{\bar{S}*(p-1),j}]$$

Because $f_{0,j}$ will never contribute to $f_{1,j}$, $f_{0,j}$ (negative infinite) is always error-free(f_0 in Fig2e top left). Then we calculate the whole matrix by equation 5 and 6. Because $f_{0,j}$ is error-free, $f_{1,j}$ to $f_{\bar{S},j}$ is correct(f_1 to f_4 in Fig2e). We save the last register $MF_{\bar{S},j}$:
202
203
204
205

$$MF_{\bar{S},j} = [f_{\bar{S},j}, f_{\bar{S}*2,j}, f_{\bar{S}*3,j}, \dots, f_{\bar{S}*p,j}]$$

Note that we calculate $f_{i+1,j}$ in equation 6, so $MF_{\bar{S},j}([f_4 f_8 f_{12} f_{16}]$ in Fig2e) is the last register to store f instead of $MF_{\bar{S}-1,j}$. Because $MF_{\bar{S},j}$ is calculated by $MF_{\bar{S}-1,j}$, it solves the problems that $f_{Y*\bar{S}+\bar{S}-1,j}$ may update $f_{Y*\bar{S}+\bar{S},j}$ ($Y = 0, 1, 2, \dots$, FigS1b).
206
207
208
209

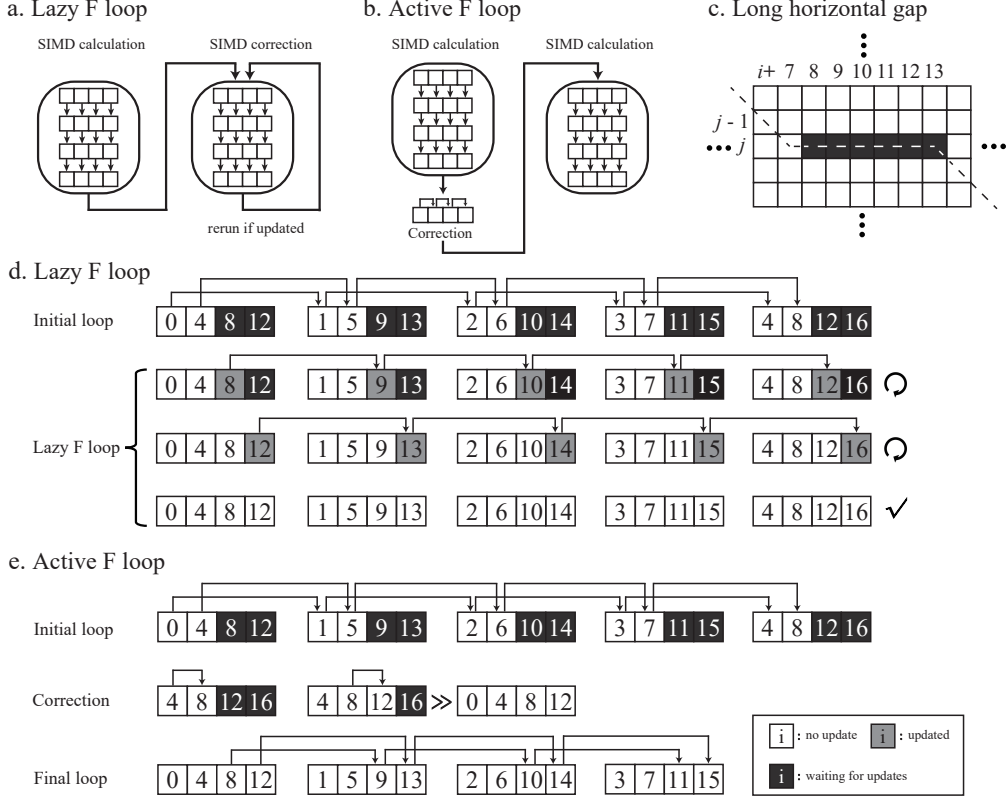


Figure 2: **The lazy and active F loop algorithm inside a row.** Assuming the band width, the number of divided segments(S) and the number of cells(p) in a register are 16, 4 and 4, respectively. (a) and (b) are the work flow for the lazy and active F loop, respectively. (c) is an example of long horizontal gap($f_{7,j}$ to $f_{13,j}$). The dash line indicates the optimal path. (d) and (e) show how the lazy and active F loop solve the above example for each cell. Black box(waiting for updates) indicates the value is influenced by F and needs to be corrected. Grey box(updated) indicates the value is updated recently. White box(no update) indicates the value is the same as expected and correct. The arrows above digits indicate the first time being updated as the correct value. (d) *Initial loop*: All the cells in the first register are negative infinity. The algorithm calculates all the cells by standard SIMD calculation. *Lazy F loop*: The algorithm keeps correcting all the registers one by one until none of them is updated. This figure shows a situation that it takes 3 loops to guarantee that all the cells are corrected. (e) Unlike the lazy F loop, there is no difference between "updated" and "no update". All the value is updated one times only. *Initial loop*: The same as the lazy F loop. *Correction*: Each cell in the first segment is checked by equation 7 and updated by the correct value. This extended register is also the first register (after the right shift) in the striped format. *Final loop*: When the first register is totally correct, the remaining segments are correct by SIMD calculation.

The only exception is that the horizontal gap is long enough to penetrate all the $f(f_{Y*\bar{S}}, f_{Y*\bar{S}+1}, \dots, f_{Y*\bar{S}+\bar{S}-1})$ in the same cell position for all registers(Fig2c,S1c). If the F penetration happens, the value of $f_{x,j}$ is smaller than $f_{x-\bar{S},j} + gappenalty$ (FigS1c). So we update the $f_{x,j}$ as the corrected value in advance when we know F penetration has happened(correction in Fig2e). The equation to update all the f in the first register $MF_{0,j}$ is following:

$$f_{x,j} = \max \begin{cases} f_{x,j} \\ f_{x-\bar{S},j} + \bar{S} * gapE - (H_{x-1,j-1} - H_{x-1-\bar{S},j-1}) \end{cases} \quad x \in (\bar{S}, \bar{S}*2, \dots \bar{S}*(p-1)) \quad (7)$$

Now, the updated f solves the problems that $f_{x-\bar{S},j}$ may update $f_{x,j}$. So $f_{Y*\bar{S}+\bar{S},j} (Y = 1, 2\dots)$ is corrected(f_8, f_{12} in Fig2). We right shift the last register $MF_{\bar{S},j}$ x bytes (length of $f_{0,j}$) and update as the first register $MF_{0,j}([f_4 f_8 f_{12} f_{16}])$ to $[f_0 f_4 f_8 f_{12}]$ in Fig2). After the active F loop, we use the updated f as the initial value and recalculate all the values by equation 5,6(final loop in Fig2e). So the remaining values are corrected ($f_5, f_9, f_{13}, f_2, f_6, f_{10}, f_7, f_{11}, f_{15}$ in Fig2 bottom). When all the values in f are corrected or error-free, all the values of H are corrected.

Specifically, the active F loop and the parallel scan in parasail[18, 19] are similar in general. One of the improvements is that the active F loop is implemented in difference recurrence relation, while the parallel scan[18] is implemented in the tradition way, storing and calculating the absolute values. Therefore, the active F loop can increase the number of parallelisms.

2.7. Edit distance

Calculating two sequences' edit distance can be regarded as a special case of pairwise alignment when the mismatch and gap extend are both equal to 1 and, the match and gap open are both equal to 0. Since the difference between adjacent cells belongs to $(-1, 0, 1)$, the number of bits for storing them is only 2. We can further increase the number of parallelisms using striped SIMD difference recurrence relation. As the number of bits decreases to 2, all the conditions can be enumerated. We converted the equation 5 and 6 to boolean logic to further accelerate the calculation.

To simplify the standard pairwise alignment, we only require H , h , u and

240 $v.$

$$\begin{cases} u_{i,j} = h_{i,j} - v_{i-1,j}, & \in (-1, 0, 1) \\ v_{i,j} = h_{i,j} - u_{i,j-1}, & \in (-1, 0, 1) \\ h_{i,j} = \min\{S_{i,j}, v_{i-1,j} + 1, u_{i,j-1} + 1\}, & \in (0, 1) \end{cases} \quad (8)$$

241 To minimize the computation resource, we defined a 2-bit binary code
 242 for boolean logic. For $h_{i,j}$, $u_{i,j}$ and $v_{i,j}$, "-1,0,1" is converted to "10,00,01".
 243 For $S_{i,j}$, "0,1" is converted to "01,00". All the conditions for calculating $h_{i,j}$
 244 from $S_{i,j}$, $u_{i,j-1}$ and $v_{i-1,j}$ is enumerated as below(Table1). The new codes
 are inside the parentheses.

$S_{i,j}(\bar{S}_{i,j}^0 \bar{S}_{i,j}^1)$	$u_{i,j-1}(\bar{u}_{i,j-1}^0 \bar{u}_{i,j-1}^1)$	$v_{i-1,j}(\bar{v}_{i-1,j}^0 \bar{v}_{i-1,j}^1)$	$=$	$h_{i,j}(h_{i,j}^0 h_{i,j}^1)$
0(01)	-1(10)	-1(10)	=	0(00)
0(01)	-1(10)	0(00)	=	0(00)
0(01)	-1(10)	1(01)	=	0(00)
0(01)	0(00)	-1(10)	=	0(00)
0(01)	0(00)	0(00)	=	0(00)
0(01)	0(00)	1(01)	=	0(00)
0(01)	1(01)	-1(10)	=	0(00)
0(01)	1(01)	0(00)	=	0(00)
0(01)	1(01)	1(01)	=	0(00)
1(00)	-1(10)	-1(00)	=	0(00)
1(00)	-1(10)	0(00)	=	0(00)
1(00)	-1(10)	1(01)	=	0(00)
1(00)	0(00)	-1(10)	=	0(00)
1(00)	0(00)	0(00)	=	1(01)
1(00)	0(00)	1(01)	=	1(01)
1(00)	1(01)	-1(10)	=	0(00)
1(00)	1(01)	0(00)	=	1(01)
1(00)	1(01)	1(01)	=	1(01)

Table 1: **In edit distance mode, enumeration of conditions for converting $h_{i,j}$ from $S_{i,j}$, $u_{i,j-1}$ and $v_{i-1,j}$.** The new binary codes are inside the parentheses.

245

246 Hence, the boolean logic for the new $\bar{h}_{i,j}$ is following:

$$\bar{h}_{i,j}^0 = 0 \quad \bar{h}_{i,j}^1 = \neg(\bar{S}_{i,j}^1 | \bar{u}_{i,j-1}^0 | \bar{v}_{i-1,j}^0) \quad (9)$$

247

248 All the conditions for calculating $u_{i,j}$ from $h_{i,j}$ and $v_{i-1,j}$ is enumerated
 as below(Table2).

$h_{i,j}(h_{i,j}^0 h_{i,j}^1)$	$v_{i-1,j}(\bar{v}_{i-1,j}^0 \bar{v}_{i-1,j}^1)$	=	$u_{i,j}(\bar{u}_{i,j}^0 \bar{u}_{i,j}^1)$
0(00)	0(00)	=	0(00)
0(00)	1(01)	=	-1(10)
0(00)	-1(10)	=	1(01)
1(01)	0(00)	=	1(01)
1(01)	1(01)	=	0(00)

Table 2: **In edit distance mode, enumeration of conditions for converting $u_{i,j}$ from $h_{i,j}$ and $v_{i-1,j}$.** The new binary codes are inside the parentheses.

As $h_{i,j} - v_{i-1,j} \in (0, 1)$, the condition of " $h_{i,j} = 1$ and $v_{i-1,j} = -1$ " does not exist. Since $v_{i,j}$ is symmetry to $u_{i,j}$ in this definition, the boolean logic for $\bar{u}_{i,j}$ and $\bar{v}_{i,j}$ is following:

$$\begin{aligned} \bar{u}_{i,j}^0 &= \bar{v}_{i-1,j}^1 \& (\neg \bar{h}_{i,j}^1) & \bar{u}_{i,j}^1 = \bar{v}_{i-1,j}^1 \wedge (\bar{h}_{i,j}^1 | \bar{v}_{i-1,j}^0 | \bar{v}_{i-1,j}^1) \\ \bar{v}_{i,j}^0 &= \bar{u}_{i,j-1}^1 \& (\neg \bar{h}_{i,j}^1) & \bar{v}_{i,j}^1 = \bar{u}_{i,j-1}^1 \wedge (\bar{h}_{i,j}^1 | \bar{u}_{i,j-1}^0 | \bar{u}_{i,j-1}^1) \end{aligned} \quad (10)$$

3. Experimental design

We implemented BSAlign with two modes: "align mode" for pairwise alignment by score matrix, and "edit mode" for pairwise alignment by minimum edit distance. For "align mode", we compared BSAlign to three striped-SIMD programs: SSW[11](version:1.0), parasail[19](version:2.4.3), ksw2[15](version:current), WFA[17](version:v2.2) and BA[16](version:0.2.0). Note that ksw2 implemented the difference recurrence relation[12] and was a component of minimap2[15]. The scores for the match, mismatch, gap open, and gap extension were set at 2, -4, -4, -2 for all implementations, respectively. For "edit mode", we compared BSAlign to Myers[20](version:myers-agrep) and Edlib[21](version:1.2.6). BA was run by rust WASM 128 bits; block size range from 32 to 2048 bp. Myers's bit-vector algorithm was one of the fastest deterministic alignment algorithms, but it did not support global alignment and did not trace back the optimal path. Edlib extended Myers's bit-vector algorithm with additional methods and traced back the optimal path.

We use the same real datasets as BA[16]. The short read dataset is 100,000 pairs of 101 bps Illumina HiSeq 2000 reads(accession number ERX069505). The long read dataset is 12,477 pairs of around 1000

271 bps Oxford Nanopore MinION reads (accession numbers ERR3278877 to
272 ERR3278886).

273 We simulated query sequences and reference sequences following a config-
274 uration that approximated the error rate in the real dataset for benchmark-
275 ing. We randomly selected 100 start positions that contained no gap within
276 a 100 kb region from GRCh38. We benchmarked software in three ways:
277 time for length, time and accuracy for divergence and length, and accuracy
278 for long indel and band width. In the time to length comparison, we set the
279 reference sizes as 10^2 , $10^{2.25}$, $10^{2.5}$, $10^{2.75}$, 10^3 , $10^{3.25}$, $10^{3.5}$, $10^{3.75}$, 10^4 , $10^{4.25}$,
280 $10^{4.5}$, $10^{4.75}$ and 10^5 base pairs with rounding. Then, we use PbSim2[22] to
281 simulate a query sequence for each reference region. These query sequences
282 and their reference sequences became pairs of input data in pairwise align-
283 ment. Sequences were simulated for both Pacbio and Nanopore using hmm
284 model P6C4 and R103. The similarity and mutation ratio (in the format of
285 substitution:insertion:deletion) are set as default value in PbSim2 (85% and
286 PacBio 6:50:54, Nanopore 23:31:46). In the time and accuracy for different
287 divergence and length comparison, we set the reference size as 10^2 , 10^3 , 10^4
288 and 10^5 base pairs. For each reference size, we also simulated reads with
289 difference divergence (80%, 95% and 99%). In the accuracy to long indel and
290 band width, the reference size is 10^4 base pairs and the divergence is 80%.
291 We randomly inserted or deleted 50, 100 and 200 base pairs sequences in the
292 middle of the reference. For each indel size, we benchmarked software with
293 different band width sizes (32, 64, 128, 256, 512 and 1024 base pairs).

294 4. Results

295 We developed the above algorithms under x86 processors using AVX2
296 SIMD and tested these programs on a machine with an AMD EPYC 7H12
297 processor, 1TB RAM, and Ubuntu Linux 20.04.1. The execution time was
298 calculated as the sum of user and system time in a single thread. We re-
299 peated each alignment experiment 1000 times in repeat mode. To achieve
300 a fair comparison, we modified the implementations to add a repeat mode
301 in SSW[11] and Myers[20]. However, we were unable to add a repeat mode
302 for parasail[19]. We developed a standard Needleman-Wunsch implemen-
303 tation to evaluate the alignment accuracy. SSW[11] performed local alignment
304 instead of global alignment, we also develop a Smith-Waterman implemen-
305 tation to evaluate SSW's accuracy. The recall rate was defined as the per-
306 centage of alignments that was the same score as the Needleman-Wunsch or

Smith-Waterman implementation for global or local alignment, respectively. 307
which may trim the tip sequence and get a higher score in comparison. We 308
also recorded the maximum memory in the system during the software exe- 309
cution. Overall, BSAlign outperformed all the other programs or was on par 310
with the best program in all of the experimental scenarios. 311

4.1. Evaluation on real data 312

Table3 showed the time and accuracy performance results for 5 algorithms 313
evaluated using both real and simulated datasets. In the case of processing 314
real datasets, BSAlign was the only algorithm that maintain 100% recall 315
rate for two datasets. WFA was the fastest algorithm for Illumina reads. 316
In "no band" mode, all algorithms aligned the whole sequences without any 317
band width. BSAlign was 1.5-5.5X times as fast as ksw2 and SSW for Ox- 318
ford Nanopore read. In "band" mode, all algorithms can align part of 319
sequences associated with the best alignment according to its method. BA was 320
the fastest algorithm for Oxford Nanopore reads with a recall rate of 87%. 321
BSAlign was the second fastest algorithm with a recall rate of 100%. Overall, 322
BSAlign was the fastest algorithm with the best recall rate for the Oxford 323
Nanopore dataset. 324

4.2. Evaluation of time and accuracy for different lengths 325

We evaluated all software in three different ways: the running time for 326
different lengths, the running time and accuracy for different divergences 327
and read lengths, and finally the accuracy for different sizes of indel and 328
different band widths. In pairwise alignment experiments, BSAlign ran faster 329
than ksw2[15], SSW[11], and parasail[19] in both "No Band" and "Band" 330
modes(Table 3 and Figure 3a). Among all algorithms trailed, only BSAlign 331
and WFA[17] have the capacity to align sequences up to 100 kbps in length. 332
Block aligner[16] was at most 3.36 times as fast as bsalign for 1,000 bps 333
sequences. When the sequence length was equal to or longer than 10,000 334
bps, bsalign was at most 1.20 to 5.61 times as fast as block aligner and other 335
algorithms. 336

4.3. Evaluation for edit distance mode 337

For the edit distance implementation, BSAlign recorded the fastest speed 338
compared to Myers[20] and Edlib[21](Figure 3b). The implementations were 339
compared in two modes. In the "whole mode", all the aligners searched the 340
whole sequences for the minimum edit distance. In the "limit mode", the 341

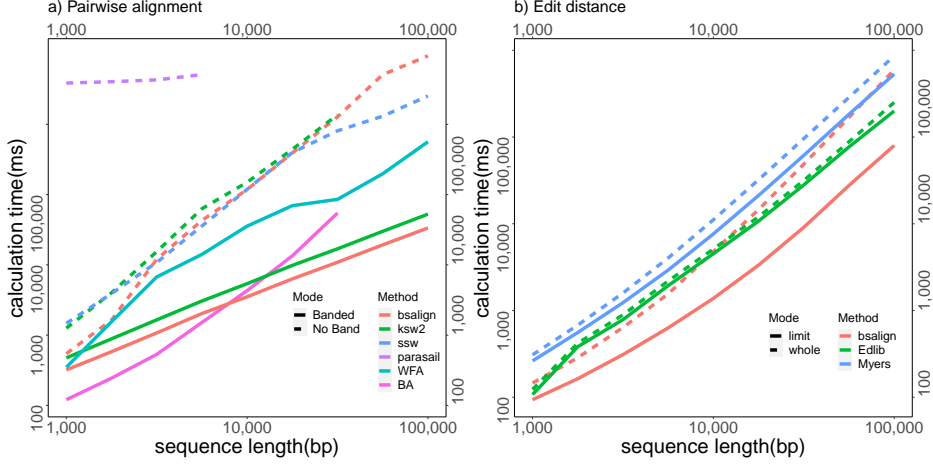


Figure 3: The average computation time in microseconds for Pairwise alignment and Edit distance. The length of the query sequence pair is from 1,000 to 100,000. Each pair is run 100 times. In **a**, six implementations: BSAAlign, ksw2[15], SSW[11], parasail[19], wavefront alignment[17] and block aligner[16] are compared. Option band width is set at 128 for BSAAlign and ksw2. In **b**, three implementations: BSAAlign, Edlib[21] and Myers[20] are compared. The mode "whole" and "limit" mean the maximum edit distance is set at the whole query length and the true edit distance in simulation, respectively.

342 minimum edit distance was specified. All the aligners were instructed to stop
 343 searching the sequences that were over the minimum edit distance. In the
 344 "whole mode", Figure3b showed that the fastest implementation switched be-
 345 tween BSAAlign and Edlib in different sequence lengths. In the "limit mode",
 346 all the aligners ran faster than the "whole mode" due to smaller searching
 347 space, where BSAAlign, Myers, and Edlib were 2.1, 1.33, and 1.11 times faster
 348 on average, respectively. BSAAlign ran 2.49 and 4.93 times as fast as My-
 349 ers and Edlib, respectively. Additionally, BSAAlign in edit distance mode is
 350 always faster than all the pairwise alignment tools.

351 *4.4. Evaluation of time and accuracy for different divergence*

352 Furthermore, we benchmarked this six software for time and accuracy
 353 performance under different divergences (Table4). The accuracy of most
 354 software was 100%, except for the small size of band width for high divergence
 355 sequences. Most software's time was stable in terms of processing time for
 356 different divergences except WFA[17]. Its time for high divergence sequences
 357 (20%) was 4.2 to 14.8 times slower than low divergence sequences'. When the
 358 length was 1000 bps, WFA and BA are fast and accurate. When the length

		Real-Illumina		Real-Ont		l=1k,d=5%		l=10k,d=5%		l=100k,d=5%		indel=50,d=20%	
		Time	Recall	Time	Recall	Time	Recall	Time	Recall	Time	Recall	Time	Recall
NoBand	bsalign	1.65	1.00	3.78	1.00	0.85	1.00	70.00	1.00	3972.13	1.00	46.21	1.00
	ksw2	1.48	0.98	9.45	1.00	2.22	1.00	207.00	1.00	error	error	171.15	1.00
	SSW	2.71	1.00	24.55	1.00	2.13	1.00	175.00	1.00	2000.22	0.00	201.33	1.00
Band	bsalign(128)	2.60	1.00	1.92	1.00	0.37	1.00	3.72	1.00	40.70	1.00	2.71	1.00
	ksw2(128)	1.82	0.98	2.79	1.00	0.58	1.00	5.98	0.78	63.30	0.02	5.01	0.00
	WFA	0.27	0.99	2.96	0.99	1.18	1.00	11.64	1.00	228.13	1.00	75.80	0.46
	WFA.score	0.12	0.99	1.85	0.99	0.85	1.00	1.18	1.00	50.39	1.00	5.21	0.46
	BA	2.16	0.99	0.91	0.87	0.11	1.00	4.48	1.00	error	error	7.57	0.00

Table 3: **Time and accuracy performance of pairwise alignment algorithms.** WFA.score only computes the alignment score, not the complete alignment.

		l=1k,d=1%		l=1k,d=5%		l=1k,d=20%		l=10k,d=1%		l=10k,d=5%		l=10k,d=20%		l=100k,d=1%		l=100k,d=5%		l=100k,d=20%	
		Time	Recall	Time	Recall	Time	Recall	Time	Recall	Time	Recall	Time	Recall	Time	Recall	Time	Recall	Time	Recall
NoBand	bsalign	0.87	1.00	0.85	1.00	0.76	1.00	70.70	1.00	70.00	1.00	62.50	1.00	91.60	1.00	92.00	1.00	81.10	1.00
	ksw2	2.25	1.00	2.22	1.00	2.01	1.00	209.00	1.00	207.00	1.00	186.00	1.00	error	error	error	error	error	error
	SSW	2.00	1.00	2.13	1.00	2.60	1.00	169.00	1.00	175.00	1.00	197.00	1.00	39.30	0.00	39.30	0.00	52.00	0.00
Band	parasail	4286.00	1.00	4394.00	1.00	4273.00	1.00	6316.16	1.00	6293.77	1.00	6086.47	1.00	error	error	error	error	error	error
	bsalign(128)	0.38	1.00	0.37	1.00	0.37	1.00	3.72	1.00	3.72	1.00	3.64	1.00	40.30	1.00	40.70	1.00	39.80	0.89
	ksw2(128)	0.57	1.00	0.58	1.00	0.55	1.00	6.06	0.77	5.98	0.74	5.59	0.00	63.70	0.27	63.30	0.02	59.70	0.00
	WFA	0.10	1.00	1.18	1.00	1.63	1.00	8.70	1.00	11.64	1.00	36.84	1.00	181.50	1.00	228.13	1.00	1156.01	1.00
	BA	0.11	1.00	0.11	1.00	0.11	1.00	4.52	1.00	4.48	1.00	4.10	1.00	error	error	error	error	error	error

Table 4: **Time(ms) and accuracy performance for different divergence.***Due to the higher deletion rate in simulation, the total sequence length of 20% divergence are 4.2% and 4.6% shorter than 5% and 1% divergence's on average, respectively.

increase to 10,000 bps, BSAlign(band width 128) is always fastest than other software. When the length further increased to 100,000 bps, BA(capacity overflow), parasail(early termination) and ksw2(core dumped) collapsed due to memory limitation. BSAlign(band width 128) was reliable and 6.70 times faster than other software.

359
360
361
362
363

4.5. Comparison of indel size, band width and accuracy

364
365
366
367
368
369
370
371
372
373
374

Because the banded methods might miss the optimal path, we further evaluated the influence of indel size on the alignment accuracy(Table5). In this context, we randomly inserted or deleted 50, 100 and 200 bp sequences in the middle of a reference(length=10k, divergence=20%). Overall, ksw2, SSW and BSAlign in "no band" mode were 100% correct. In band mode, WFA detected approximately 50% long indels while BA detected none. ksw2 detected all the indels when the band width was set at 1024 bps. BSAlign with band width 128, 256 and 512 bps detected all the 50, 100 and 200 bps indels, respectively. As expected, to accurately detect long indels, the band width size should be two times larger than the indel size. It suggests that

		indel=50,d=20%		indel=100,d=20%		indel=200,d=20%	
		Time	Recall	Time	Recall	Time	Recall
No Band	bsalign	46.21	1.00	45.93	1.00	45.49	1.00
	ksw2	171.15	1.00	171.04	1.00	171.00	1.00
	SSW	121.90	0.99	127.88	0.99	153.19	0.99
Band 128 bp	bsalign	2.71	1.00	2.65	0.01	2.64	0.00
	ksw2	5.01	0.00	5.10	0.11	4.90	0.15
Band 256 bp	bsalign	3.26	1.00	3.30	1.00	3.22	0.00
	ksw2	9.51	0.43	9.46	0.42	9.28	0.38
Band 512 bp	bsalign	4.66	1.00	4.65	1.00	4.62	1.00
	ksw2	18.15	1.00	18.21	0.98	18.03	0.83
Band 1024 bp	bsalign	9.03	1.00	9.03	1.00	8.87	1.00
	ksw2	35.16	1.00	35.12	1.00	34.69	1.00
Band	WFA	75.80	0.46	75.08	0.51	76.14	0.61
	BA	7.57	0.00	7.47	0.00	7.48	0.00

Table 5: Time(ms) and accuracy for difference indel size(50,100 and 200 bp) and band size(128 to 1024 bp).

375 BSAAlign’s striped move is the most accurate strategy to find the optimal
 376 path. Regarding the speed, BSAAlign is always faster than others. Notably,
 377 the lazy F loop implementation SSW[11] run slower for long indels while the
 378 active F loop implementation BSAAlign’s runtime was stable for all the indel
 379 sizes. It suggests that BSAAlign’s active F loop is fast and stable.

380 4.6. Comparison about memory

381 We also measured the memory during the execution(Table6). All the soft-
 382 ware except WFA required similar memory for difference divergence. The
 383 memory increased as the sequence length increased. No band method re-
 384 quired a larger memory as they stored and calculated the whole alignment
 385 matrix. The banded method required less memory than other methods. For
 386 example, BSAAlign (band width 128 bps) required 16.36 and 32.46 times less
 387 memory than WFA and BA for length 10k and divergence 20%, respectively.

388 5. Discussion and Conclusion

389 Designing a dynamic banding method is about seeking a balance between
 390 speed and accuracy. No software can guarantee both fast and accurate results
 391 under any conditions. For example, WFA[17] works well for low divergence

		Length=1K			Length=10K			Length=100K		
		d=1%	d=5%	d=20%	d=1%	d=5%	d=20%	d=1%	d=5%	d=20%
NoBand	bsalign	4.19	4.18	3.97	184.72	183.90	162.52	18471.66	18314.93	16433.11
	ksw2	5.16	4.91	4.56	157.56	154.53	143.79	error	error	error
	SSW	4.08	4.43	7.07	10.57	11.82	17.94	24.19	27.56	140.14
Band	bsalign(128)	2.54	2.52	2.50	5.89	5.88	5.65	40.35	40.18	36.86
	ksw2(128)	2.13	2.09	2.05	6.80	6.31	7.53	33.14	33.11	31.19
	WFA	8.58	10.39	10.61	37.41	35.00	98.08	153.52	217.70	2095.99
	BA	172.20	175.53	177.19	189.66	189.27	189.04	error	error	error

Table 6: **Memory (Mb) for difference size and divergence.**

short sequences. BA[16] and ksw2[15] work well for high divergence short sequences. When the sequences are short, the band width is short as well. In this case, data structure like striped SIMD is unnecessary and time-wasting. When the sequences are long (10k bps or more), the band width increases as well. In this case, the data structure like striped SIMD is necessary and fast. The striped SIMD banded method BSAlign is faster than the anti-diagonal banding method ksw2 when the band width is 128 bps($p = 16, S_{bar} = 4$ in 128 SSE).

392
393
394
395
396
397
398
399
400

Appendix A. Availability of source code and requirements

Lists the following:

- Project name: BSAlign
- Project home page: <https://github.com/ruanjue/BSAlign>
- Operating system(s): Linux
- Programming language: C Language
- Other requirements: None
- License: GNU General Public License v3.0

401
402
403
404
405
406
407
408

Appendix B. Declarations

Appendix B.1. List of abbreviations

SW:Smith-Waterman
SIMD:single instruction multiple data
DP:dynamic programming

409
410
411
412
413

414 *Appendix B.2. List of symbols*

415 Q : Query sequence.

416 R : Reference sequence.

417 S : Matching matrix.

418 H : Alignment score.

419 h : difference of H .

420 E : Alignment score end with a vertical gap.

421 e : difference of E .

422 F : Alignment score end with a horizontal gap.

423 f : difference of F .

424 $GapO$: gap open, less than zero.

425 $GapE$: gap extension, less than zero.

426 $GapOE$: $GapO + GapE$.

427 S : The number of divided segments(for whole query sequence).

428 \bar{S} : The number of divided segments(for band width).

429 p : The number of segments in a SIMD register.

430 N : register(for any value).

431 M : register in striped order(for any value).

432 MF : register in striped order(for f).

433 i : column id.

434 j : row id.

435 $u_{i,j}$: vertical difference between $H(H_{i,j} - H_{i-1,j})$.

436 $v_{i,j}$: horizontal difference between $H(H_{i,j} - H_{i,j-1})$.

437 \bar{h} : h in new code for edit distance mode.

438 \bar{u} : u in new code for edit distance mode.

439 \bar{v} : v in new code for edit distance mode.

440

441 *Appendix B.3. Consent for publication*

442 Not applicable.

443 *Appendix B.4. Competing Interests*

444 The authors declare that they have no competing interests.

445 *Appendix B.5. Funding*

446 This study was supported by the National Key Research and Develop-
447 ment Project Program of China (2019YFE0109600) and the National Natural
448 Science Foundation of China (31822029 and 32200517).

<i>Appendix B.6. Author's Contributions</i>	449
J.R. conceived the project, designed the algorithm, and implemented BSAlign. H.S. contributed to the development and drafted the manuscript. Both authors evaluated the results and revised the manuscript.	450 451 452
Appendix C. Acknowledgements	453
We thank Shigang Wu from CAAS for the help in the sequence alignment comparison. We thank Fan Zhang from CAAS for the help in manuscript preparation.	454 455 456
References	457
[1] S. B. Needleman, C. D. Wunsch, A general method applicable to the search for similarities in the amino acid sequence of two proteins, <i>Journal of Molecular Biology</i> 48 (3) (1970) 443–453.	458 459 460
[2] T. Smith, M. Waterman, Identification of common molecular subse- quences., <i>Journal of Molecular Biology</i> 147 (1) (1981) 195–197.	461 462
[3] A. Wozniak, Using video-oriented instructions to speed up sequence comparison, <i>Bioinformatics</i> 13 (2) (1997) 145–150.	463 464
[4] T. Rognes, E. Seeberg, Six-fold speed-up of smith-waterman sequence database searches using parallel processing on common microprocessors, <i>Bioinformatics</i> 16 (8) (2000) 699–706.	465 466 467
[5] J. Zhang, H. Lan, Y. Chan, Y. Shang, B. Schmidt, W. Liu, BGSA: a bit-parallel global sequence alignment toolkit for multi- core and many-core architectures, <i>Bioinformatics</i> 35 (13) (2018) 2306–2308. arXiv: https://academic.oup.com/bioinformatics/article-pdf/35/13/2306/28878352/bty930_supplementary_data.pdf , doi:10.1093/bioinformatics/bty930. URL https://doi.org/10.1093/bioinformatics/bty930	468 469 470 471 472 473 474
[6] R. Rahn, S. Budach, P. Costanza, M. Ehrhardt, J. Hancox, K. Reinert, Generic accelerated sequence alignment in SeqAn us- ing vectorization and multi-threading, <i>Bioinformatics</i> 34 (20) (2018) 3437–3445. arXiv: https://academic.oup.com/bioinformatics/article-pdf/34/20/3437/48918959/bioinformatics_34_20_3437_s5.pdf ,	475 476 477 478 479

480 doi:10.1093/bioinformatics/bty380.
481 URL <https://doi.org/10.1093/bioinformatics/bty380>

482 [7] A. Müller, B. Schmidt, A. Hildebrandt, R. Membarth, R. Leȋa,
483 M. Kruse, S. Hack, Anyseq: A high performance sequence
484 alignment library based on partial evaluation (2020) 1030–
485 1040doi:10.1109/IPDPS47924.2020.00109.

486 [8] M. Farrar, Striped smith–waterman speeds database searches six times
487 over other simd implementations, *Bioinformatics* 23 (2) (2007) 156–161.

488 [9] H. Li, R. Durbin, Fast and accurate short read alignment with bur-
489 rows–wheeler transform, *Bioinformatics* 25 (14) (2009) 1754–1760.

490 [10] B. Langmead, S. L. Salzberg, Fast gapped-read alignment with bowtie
491 2, *Nature methods* 9 (4) (2012) 357–359.

492 [11] M. Zhao, W. P. Lee, E. P. Garrison, G. T. Marth, Ssw library: an simd
493 smith–waterman c/c++ library for use in genomic applications., *PLOS*
494 ONE 8 (12) (2013).

495 [12] H. Suzuki, M. Kasahara, Introducing difference recurrence relations for
496 faster semi-global alignment of long sequences., *BMC Bioinformatics*
497 19 (1) (2018) 33–47.

498 [13] K.-M. Chao, W. R. Pearson, W. Miller, Aligning two sequences
499 within a specified diagonal band, *Bioinformatics* 8 (5) (1992)
500 481–487. arXiv:<https://academic.oup.com/bioinformatics/article-pdf/8/5/481/566378/8-5-481.pdf>, doi:10.1093/bioinformatics/8.5.481.
501 URL <https://doi.org/10.1093/bioinformatics/8.5.481>

502 [14] H. Suzuki, M. Kasahara, Acceleration of nucleotide semi-global align-
503 ment with adaptive banded dynamic programming, *bioRxiv* (2017)
504 130633.

505 [15] H. Li, Minimap2: pairwise alignment for nucleotide
506 sequences, *Bioinformatics* 34 (18) (2018) 3094–3100.
507 arXiv:<https://academic.oup.com/bioinformatics/article-pdf/34/18/3094/25731859/bty191.pdf>, doi:10.1093/bioinformatics/bty191.
508 URL <https://doi.org/10.1093/bioinformatics/bty191>

- [16] D. Liu, M. Steinegger, Block aligner: fast and flexible pairwise sequence alignment with simd-accelerated adaptive blocks, bioRxiv (2021). 511
512
- [17] S. Marco-Sola, J. C. Moure, M. Moreto, A. Espinosa, Fast gap-affine pairwise alignment using the wavefront algorithm, Bioinformatics 37 (4) (2021) 456–463. 513
514
515
- [18] J. A. Daily, Scalable parallel methods for analyzing metagenomics data at extreme scale, Washington State University, 2015. 516
517
- [19] J. A. Daily, Parasail: Simd c library for global, semi-global, and local pairwise sequence alignments, BMC Bioinformatics 17 (1) (2016) 81–81. 518
519
- [20] G. Myers, A fast bit-vector algorithm for approximate string matching based on dynamic programming, Journal of the ACM 46 (3) (1999) 395–415. 520
521
522
- [21] M. Šošić, M. Šikić, Edlib: a C/C++ library for fast, exact sequence alignment using edit distance, Bioinformatics 33 (9) (2017) 1394–1395. arXiv:<https://academic.oup.com/bioinformatics/article-pdf/33/9/1394/25151249/btw753.pdf>, doi:10.1093/bioinformatics/btw753 523
524
525
526
URL <https://doi.org/10.1093/bioinformatics/btw753> 527
- [22] Y. Ono, K. Asai, M. Hamada, PBSIM2: a simulator for long-read sequencers with a novel generative model of quality scores, Bioinformatics 37 (5) (2020) 589–595. arXiv:<https://academic.oup.com/bioinformatics/article-pdf/37/5/589/37809062/btaa835.pdf>, doi:10.1093/bioinformatics/btaa835 528
529
530
531
532
URL <https://doi.org/10.1093/bioinformatics/btaa835> 533

Appendix A. Supplementary Figures

534

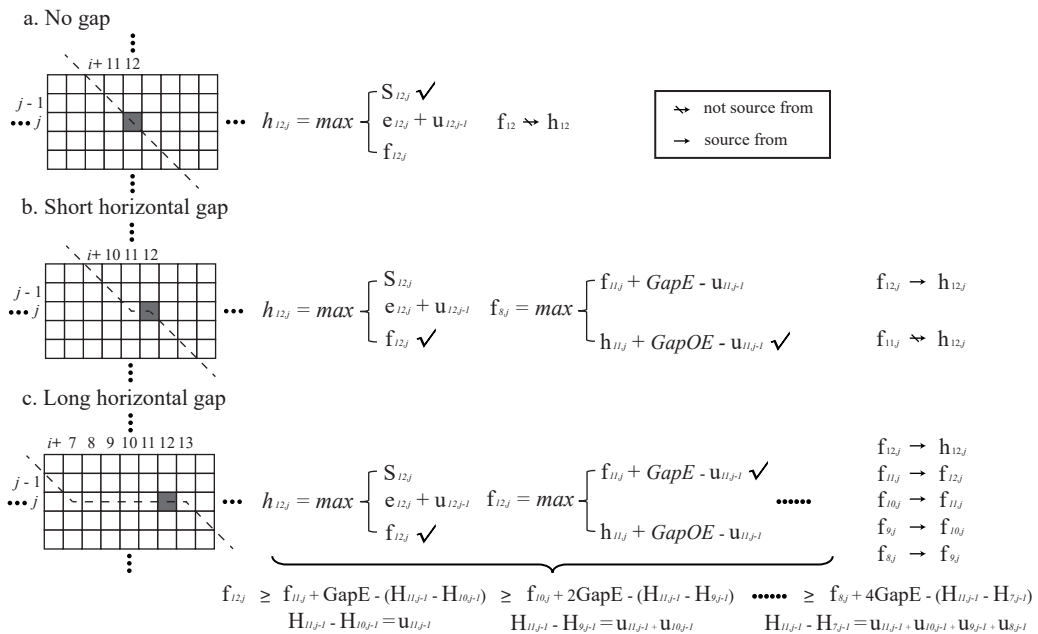


Figure S1: **The F loop in non-striped order.** (a-c) shows how the pairwise alignment calculates a cell ($h_{12,j}$) in non-striped order in three situations: (a) no gap, (b) short horizontal gap and (c) long horizontal gap. The dash line indicates the optimal path.